Electronic Supplementary Material (ESI) for Nanoscale.

Supporting Information for

Enhancement of Exciton Transport in Porphyrin Aggregate Nanostructures by Controlling Hierarchical Self-Assembly

*Taehee Kim, Sujin Ham, Sang Hyeon Lee, Yongseok Hong, Dongho Kim**

Spectroscopy Laboratory for Functional π-Electronic Systems and Department of Chemistry, Yonsei University, Seoul 03722, Korea

Contents

1. Sample preparation methods of TPPS aggregates

Meso-tetra(4-sulfonatophenyl) porphyrin (TPPS) was purchased from Sigma Aldrich. Bulk solution was first prepared in deionized water with concentration of 2 mM. It was diluted 100 times to produce 20 μM solution. Minuscule amount of 1.0 M hydrochloric acid was added to adjust the pH of solution to ~3.0. The purple colored solution then turned green, indicating the transition of tetra-anion form monomer to diacid form monomer. This 20 μM solution was mixed with 1.5 M NaCl and CsCl solutions in 1:1 ratio, to induce aggregation. Upon aggregation, the solution turned into yellowish-green color. The solution was kept for at least 1 hr for the complete aggregation. For direct comparison in measuring absorption spectra (Figure 2), diacid monomer solution was diluted to identical concentration (10 μM) and pH adjusted to 3.0.

For confocal microscopy experiment, prepared 10 μM solution of TPPS with 0.75 M CsCl and 0.75 M NaCl were each deposited on cleaned coverslip and spin-coated for 30 s with 2000 rpm.

2. Confocal fluorescence microscopy

Confocal microscope (TE2000-U, Nikon) was equipped with a sample scanning stage at room temperature. Circular polarized light from a picosecond pulsed diode laser (LDH-P-C-485, Picoquant, 10 MHz repetition rate, prepared using a Berek compensator (5540, New Focus)) excited the samples. It was passed through a laser line filter (D485/25x, Chroma Technology) and collimating lens. Then, it subsequently focused on the sample via an oil immersion objective (Plan Fluor, 1.3 NA, 100×, Nikon). Fluorescent signals were passed through a dichroic mirror (AT485DC, Chroma Technology). While collecting the emission profile, the fluorescence signal was spectrally filtered using a notch filter (HNPF-485.0-1.0, Kaiser optical systems) and a band pass filter (HQ560LP, Chroma Technology), and while collecting the excitation laser beam profile, these two filters were flipped down. Fluorescence was dispersed via a spectrograph (SpectraPro 2150i, Princeton Instruments) and projected onto an EMCCD camera (PL PROEM:512B EMCCD, Princeton Instruments). When obtaining the fluorescence emission spectrum, the spectrograph was set at the relevant center wavelength (720 nm), and when collecting the profile images, the spectrograph was set to zero-order grating.

3. Emission profile analysis

The corresponding excitation beam profiles (panels b and f, respectively) were obtained by focusing the laser beam at the empty spots marked with yellow spots in the fluorescence scan images and collecting the reflected laser beam profiles using an electron-multiplying charge-coupled device (EMCCD). To image the spatial extent of the exciton transport, the excitation beam was focused on a selected spot on the aggregates and the resulting fluorescence emission profile was again collected using the EMCCD (Fig. 4c, 4g). The emission profiles represent the spatially resolved migration of exciton, which is averaged over time. Immediately after collecting the emission profile, the fluorescence emission spectrum was obtained at the same spot by setting the spectrograph grating at an appropriate wavelength (Fig. S1). To quantify exciton transport, exciton diffusion length was first calculated from excitation and emission profiles. Circular excitation laser beam profiles were fitted to 2D gaussian function to obtain the beam size information. Considering that the spatial distribution of singlet exciton is usually described as gaussian function, (see section. 9) the cross-section profiles were fitted to the convolution of two Gaussian probability density functions:

$$n(x) = \frac{1}{\sqrt{2\pi(\sigma_0^2+\sigma_{diffused}^2)}} e^{-\frac{(x-(x_0+x_{diffused}))^2}{2(\sigma_0^2+\sigma_{diffused}^2)}}$$

where parameter σ_0 was fixed with the value obtained from the previously fitted excitation beam profile, and $\sigma_{diffused}$ was considered as the exciton diffusion length L_D.

4. Fluorescence emission spectra of TPPS aggregates obtained using confocal microscopy

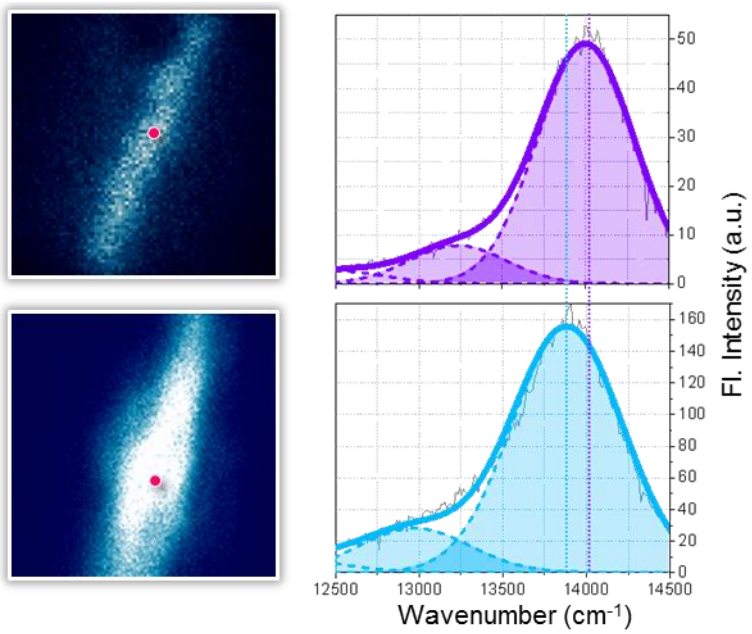

Figure S1. Representative fluorescence emission spectra obtained from the local area excitation at each aggregate structures. Nanotube (above) and bundle (below).

Right after collecting the emission profile, the fluorescence emission spectrum was obtained at the very same spot by setting the spectrograph grating at the relevant wavelength (Figure S4). Fluorescence emission spectra were fitted to Gaussian function with 2 additional replica peaks corresponding to the vibronic peaks. The area of individual 0-0 and 0-1 peaks ($I_{0\text{-}0}$ and $I_{0\text{-}1}$, respectively) were obtained from the fitted result, and were used to calculate the coherence number through formula $N_{coh} = S \cdot I_{0\text{-}0}/I_{0\text{-}1}$.

5. Determination of singlet exciton lifetimes of TPPS aggregates by TCSPC measurements

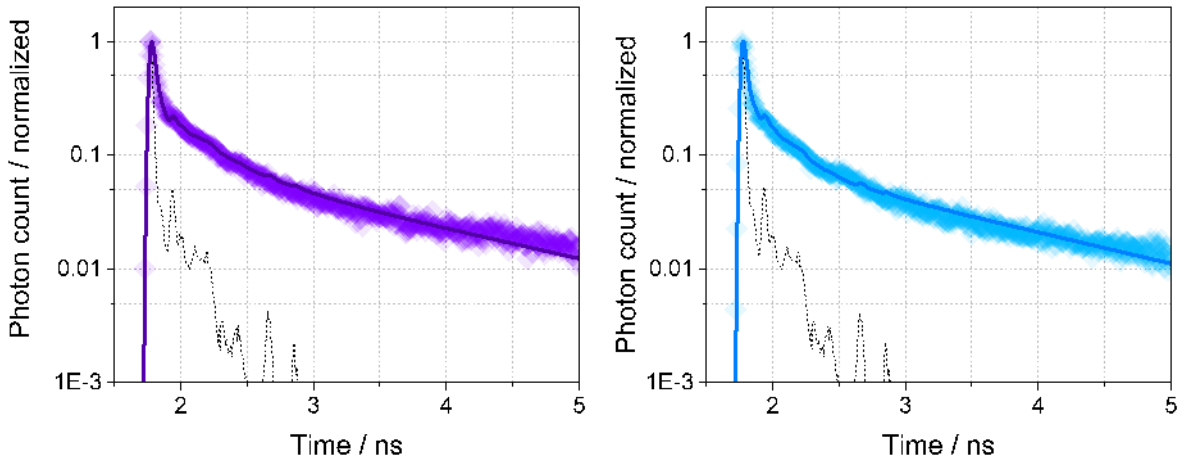

Figure S2. Fluorescence decay profiles of TPPS nanotube (left) and bundle (right).

	τ_1 (ps)	τ_2 (ps)	τ_3 (ns)
Nanotube (CsCl)	17 (0.85)	187 (0.11)	1.6 (0.03)
Bundle (NaCl)	17 (0.86)	177 (0.11)	1.6 (0.03)

Fluorescence decay profiles of nanotube and bundle were obtained by time-correlated single photon counting (TCSPC) measurements. The decay curves were both fitted with tri-exponential function, and the results are summarized in table above. The second time component was considered as the singlet exciton lifetime, in accordance with the previously reported values at hundreds of picoseconds order.

6. Statistical distribution of exciton diffusion lengths

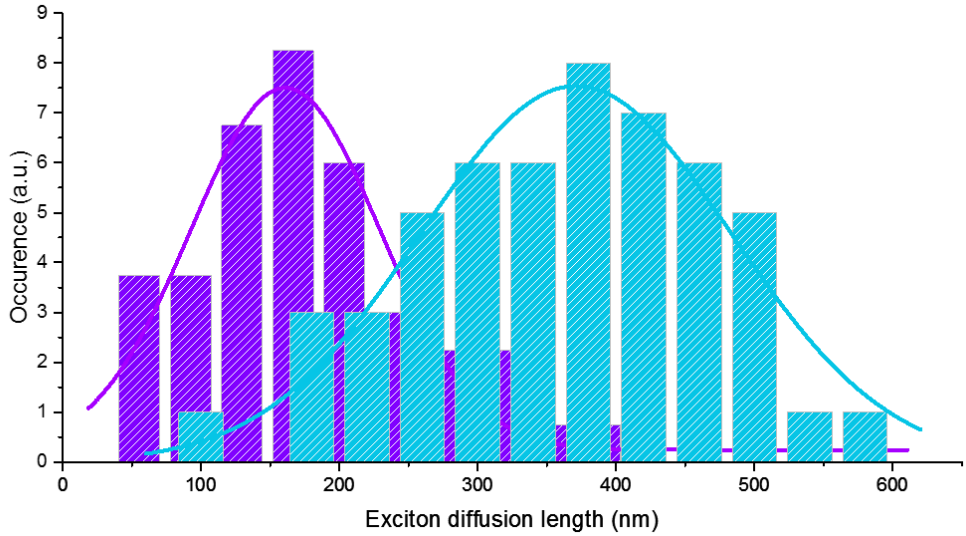

Figure S3. Statistical distribution of exciton diffusion lengths of nanotube (purple) and bundle (sky blue).

The L_D values were estimated from more than 50 spots in ~10 single nanotubes/bundles. Statistic distribution of L_D values exhibited gaussian distribution, and mean L_D value for nanotubes and bundles are 160 nm and 370 nm, respectively.

7. Correlative analysis: Lcoh vs D in single aggregates

Nanotube

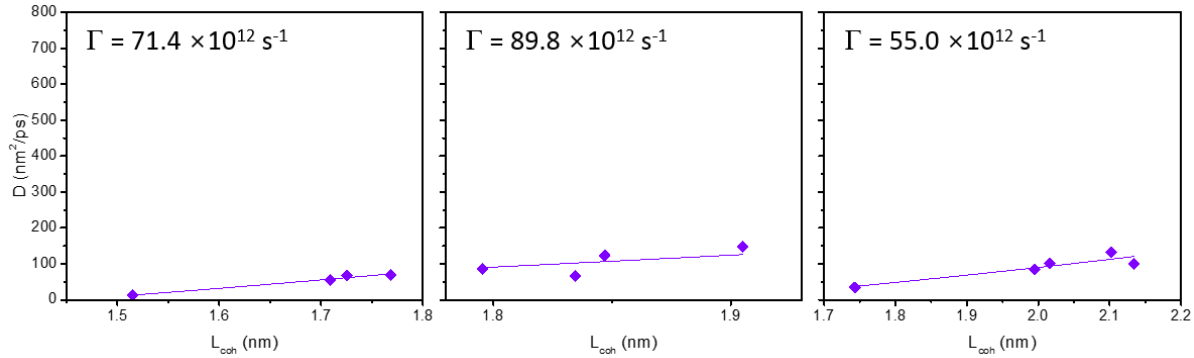

Figure S4. Scatter plots showing relationship between coherence length and diffusion coefficient in single nanotubes

Bundle

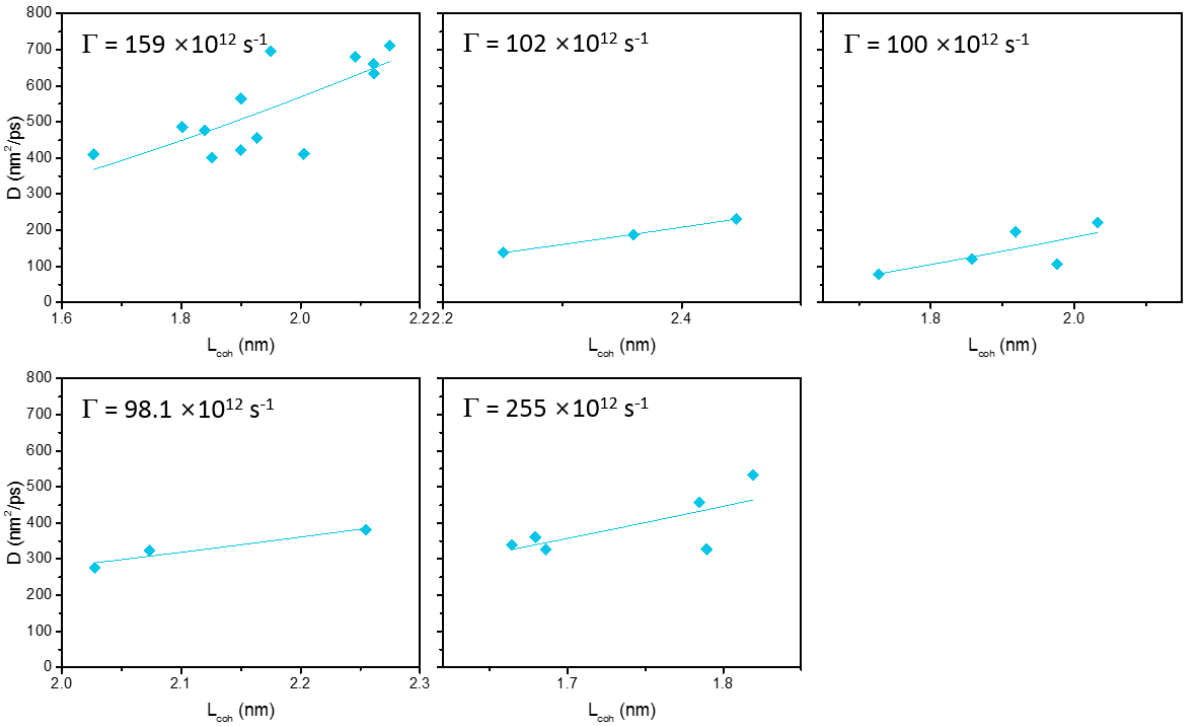

Figure S5. Scatter plots showing relationship between coherence length and diffusion coefficient in single bundles.

Relationship between coherence length and diffusion coefficient in single nanotubes/bundles. Plots were fitted with function $D = \Gamma L_{coh}^2$, and Γ values, indicating the strength of system-environment coupling are mentioned in each of the above plots.

8. Absorption band tailing

Absorption tail breadth is known to be determined by the tail breadth of the density of electronic states.[1] Absorption tail is usually described by a linear-exponential function

$$A(hv) = A_0 e^{(hv - hv_0/E_0)}$$

where A_0 and hv_0 are numerical constants, and E_0 is referred to as the absorption tail breadth.[2] The absorption tails of the Q_0 band of nanotube and bundle were fitted with the above equation to compare the absorption tail breadth E_0.

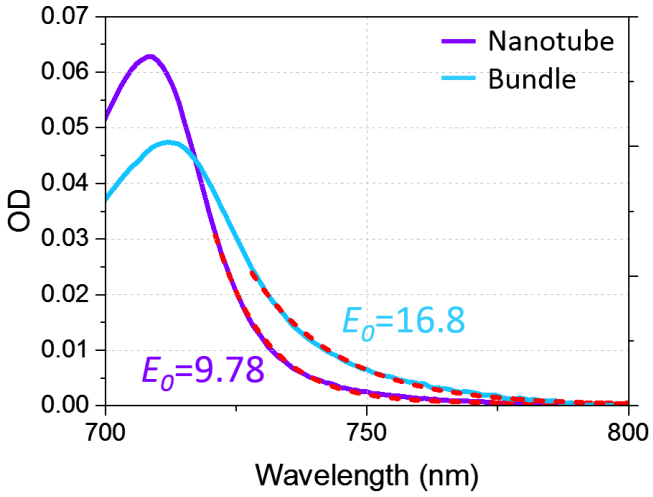

Figure S6. Absorption tails of of the Q0 band of nanotube and bundle fitted with exponential function.

The larger E_0 value obtained from bundle is a direct evidence of relatively more intense band tailing of DOS, which is fundamentally related to the disorder of the system. In this regard, we believe that the different extent of absorption red-tailing provides a reasonable experimental evidence of increased disorder and broader distribution of energy states in TPPS bundle.

9. 1D diffusion model

The one-dimensional diffusion equation for exciton density including decay to the ground state is

$$\frac{\partial n(x,t)}{\partial t} = \mathrm{D}\frac{\partial^2 n(x,t)}{\partial x^2} - \frac{n(x,t)}{\tau}$$

where *n(x,t)* is space and time dependent density of excitons, *D* is the diffusion coefficient and τ is the singlet exciton lifetime. The general solution to the above diffusion equation is

$$n(x,t) = \frac{1}{\sqrt{4\pi Dt}}\int_{-\infty}^{\infty} n(x_0,0)\exp\left[-\frac{(x-x_0)^2}{4Dt}\right]dx_0$$

with the general initial condition $n(x_0,0)$.

Here, the initial singlet exciton density *n(x,0)* is a 1D Gaussian distribution created by Gaussian excitation beam, given by $n(x,0) = N_0\exp(-x^2/2\sigma_0^2)$. Then, the singlet exciton density at later time t is

$$n(x,t) = \frac{N_0}{\sqrt{4\pi Dt}}\int_{-\infty}^{\infty}\exp\left[-\frac{x^2}{2\sigma_0^2}\right]\exp\left[-\frac{(x-x_0)^2}{4Dt}\right]dx_0$$

$$= \frac{N_0}{\sqrt{4\pi Dt}}\exp\left(\frac{x^2}{2\sigma_0^2 + 4Dt}\right)$$

According to Fick's Law, the variance of the singlet exciton distribution, which is the mean square displacement $< x(t)^2 >$, can be expressed as

$$< x(t)^2 > = \sigma^2(t) = \sigma_0^2(0) + 2Dt$$

In our experiment, the fluorescence profile image was considered as the convolution of initial singlet exciton density created by Gaussian excitation beam and the extent of exciton diffusion along the tube axis. Since the fluorescence profile was time-averaged, we considered the

process as steady-state. Then, we could substitute t in the second term on the right side of the equation above with the singlet exciton lifetime τ, the time range in which any diffusion event can take place. Using the fact that the variances of individual Gaussian functions are additive when convoluted, and that the initial Gaussian excitation beam variance is $\sigma_{beam}^2 = \sigma_0^2$, the second term $2D\tau$ can be considered as the steady-state variance of singlet exciton distribution, expressed as follows:

$$2Dt = \sigma_{emission}^2 = L_D^2$$

Reference

1. S. K. O'Leary, S.R. Johnson and P. K. Lim, The relationship between the distribution of electronic states and the optical absorption spectrum of an amorphous semiconductor: An empirical analysis. *J. App. Phys*, 1997, **82**, 3334.

2. G. D. Cody, T. Tiedje, B. Abeles, B. Brooks and Y. Goldstein, Disorder and the Optical-Absorption Edge of Hydrogenated Amorphous Silicon. *Phys. Rev. Lett*, 1981, **47**, 1480.